Int J Clin Exp Med 2019;12(9):11938-11945
www.ijcem.com /ISSN:1940-5901/IJCEM0094884

*Original Article*

# Proteomic analyses of molecular factors associated with obstructive megaureter dysfunction

Hyo Jin Kang[1,2], Ji Hee Jun[1], Sang Won Han[1]

[1]*Department of Pediatric Urology, Severance Children's Hospital, Urological Science Institute, Yonsei University College of Medicine, Seoul, Korea;* [2]*Medical Science Research Institute, Seoul National University Bundang Hospital, Seongnam, Korea*

Received April 4, 2019; Accepted June 10, 2019; Epub September 15, 2019; Published September 30, 2019

**Abstract:** Objective: The underlying pathophysiology of obstructive and refluxing megaureters is poorly understood. The current study investigated the molecular mechanisms of ureter dysfunction, identifying proteins via proteomic analyses. Materials and methods: Megaureter and normal ureter tissues were used to examine differentially-expressed proteins. Smooth muscle cells (SMCs) of obstructive megaureters were obtained from five patients that underwent open ureteroneocystostomy surgeries and five control patients with low-grade vesicoureteral reflux. SMCs were cultured in M199 medium supplemented with 10% fetal bovine serum and 1% antibiotics. Aiming to identify differentially-expressed proteins, protein spots separated by 2D gel electrophoresis were matched. They were then analyzed using PDQuest software and nanoflow LC-ESI-MS-MS. Results: In the current study, α-tropomyosin, a protein associated with the contraction and migration of SMCs, was selected from several analyzed proteins, investigating its relationship with megaureters. When TPM1 was artificially overexpressed in normal ureter SMCs, a significant change in morphology was observed. In addition, the rate of apoptosis was increased in transfected SMCs, compared to that in control SMCs. Conclusion: Abnormal overexpression of TPM1 in ureter SMCs may induce defects in contractility and increase apoptosis rates. Empty spaces caused by apoptosis may then be preferentially filled with connective tissues, rather than slowly migrating SMCs. As a result, contractility is reduced, leading to the development of a dilated ureter.

**Keywords:** Obstructive megaureter, smooth muscle cell, tropomyosin 1 (TPM1), 2D electrophoresis, proteomics

## Introduction

There are multiple classifications of megaureters, including primary or secondary, as well as obstructed, refluxing, obstructed and refluxing, and neither obstructing nor refluxing [1]. The current study focused only on cases of primary obstructing megaureters, which are typically detected as an abnormal narrowing at the vesicourethral junction. This interrupts the normal rate of urine transport and causes functional obstruction [2, 3]. Several reasons for abnormal movement have been proposed, including increased collagen ratios, abnormal development of circular muscle fibers, and loss of muscle layers [4, 5]. However, the pathology of megaureters remains controversial.

Tropomyosins (TPMs) are α-helical coiled coil dimers that form continuous polymers along the major groove of actin filaments. The TPM family of actin-binding proteins is essential for actin filament integrity. It consists of several isoforms that can be divided into three categories, striated muscles, smooth muscles, and cytoplasmic [6]. In striated muscles, TPMs participate in muscle contraction by regulating the interaction between actin and myosin. TPM1 plays an important role in $Ca^{2+}$-dependent contractions. It can occupy three unique positions on actin ("blocked" or calcium-free, "closed" or calcium-induced, and "open" or myosin-induced), depending on the presence of calcium, myosin, and troponin [7]. In addition to motility, apoptosis is important for maintenance of regular function and activities of cells. Failure of this process can lead to several pathologies. Interactions between cells and the extracellular matrix regulate apoptosis through focal adhesions and integrins [8]. TPM1 can regulate the molecular composition of microfilaments. This, in turn, regulates dynamics, functional proper-

ties, and morphologies of the resulting actin filament population [9].

In this study, because biological processes are directly regulated by proteins, proteomic analyses were used to analyze differential gene expression at the protein level, comparing the two-dimensional (2D) electrophoresis patterns of proteomes in control and megaureter smooth muscle cells (SMCs) [10].

## Materials and methods

### *Megaureter SMC isolation, primary culturing, and identification*

Megaureter SMCs were obtained from five patients with obstructive megaureters (age range: 8-20 months) that underwent open ureteroneocystostomy surgeries and five controls (age range: 12-38 months) with low-grade vesicoureteral reflux that did not exhibit ureter dilation. After being excised, the tissues were placed in 0.1% collagenase IV (Washington Biochemical Co., Lakewood, NJ, USA) and incubated at 37°C in a humidified atmosphere with 5% $CO_2$ for 1 hour. Collagenase IV was neutralized with culture media and separated by centrifugation. Supernatants then were passed through a 100 μm cell strainer (BD Bioscience, Bedford, MA) before plating. Pellets were washed in phosphate-buffered saline and seeded in M199 media (Sigma-Aldrich, St. Louis, MO, USA) with 10% fetal bovine serum (Gibco, Carlsbad, CA, USA), 100 U/mL penicillin, and 100 μg/mL streptomycin at 37°C in a humidified 5% $CO_2$ incubator. Confirming the identity of SMCs, ureter SMCs were fixed in 4% formaldehyde, permeabilized with 0.2% Triton X-100, and stained with α-SMA antibodies (1:200, Abcam, Cambridge, UK). All stained samples were imaged using an Olympus fluorescence inverted microscope (100 × magnification).

### *2D electrophoresis and spot image analyses*

SMCs were dissolved in lysis buffer and separated by immobilized pH gradient (IPG) isoelectric focusing (IEF) using a Protean IEF cell (Bio-Rad, Hercules, CA, USA). The first dimension IEF was followed by a series of steps, including 12 hours of rehydration, 15 min/250 V, 500 V·h/500 V, 1,000 V·h/1,000 V, 10,000 V·h/4,000 V, and 40,000 V·h/10,000 V. After first-dimensional separation, IPG gels were incubated in equilibration buffer I with 1% dithiothreitol for 30 minutes. They were then added with equilibration buffer II with 2.5% iodoacetamide for 30 minutes. Equilibrated IPG gels were separated on 10% SDS-polyacrylamide gels. Proteins were visualized by Coomassie blue staining. This allowed for direct correlation of the intensity of the protein spot with the quantity of protein present.

Gels were scanned using a GS-800 Calibrated Densitometer (Bio-Rad) and matched to analyze differentially-expressed spots using PDQuest software version 8.0.1 (Bio-Rad). Each matched protein spot was assigned a unique sample spot protein number in the PDQuest software. Matched spots were compared by Student's t-tests, with a 95% significance level. A minimum 10.0-fold change was considered for upregulated proteins, while a 0.1-fold change was considered for downregulated proteins.

### *Nanoflow LC-ESI-MS-MS analyses*

Nanoflow LC-ESI-MS-MS experiments were carried out using a CapLC equipped with a Q-TOF Ultima mass spectrometer (Waters, Milford, MA, USA). It used a custom-made pulled tip capillary column (75 μm i.d., 360 μm o.d., 15 cm). For each sample, 5.0 μL of the digested peptide mixture was injected via an autosampler connected to the trapping column. The flow rate during gradient separation remained at 200 nL/min and eluted peptides were directly electro-sprayed into the mass spectrometer with a spray voltage of 2.4 kV in the positive ion mode. Peptide ions were detected in the data-dependent analyses mode with an MS precursor scan (300-1700 amu). This was followed by three data-dependent MS-MS scans. For data analyses, collected raw MS/MS spectra were analyzed with the Mascot search program using NCBI databases. The accepted mass tolerance used was 100 ppm for both molar masses of the precursor peptide and peptide fragment ions. For analyses of search data, only peptides yielding Mascot ion scores > 49 indicating extensive homology were accepted.

### *Western blotting*

Western blotting was performed with mouse anti-human tropomyosin 1 (1:500, Santa Cruz, Dallas, TX, USA), mouse anti-human α-smooth

muscle actin (1:500, α-SMA, Abcam), and mouse anti-human Tm311 (1:500, Santa Cruz). Proteins were mixed with 5X sample buffer, heated at 95°C for 10 minutes, and separated on 10% SDS-polyacrylamide gels. Proteins were transferred onto membranes with the transfer buffer, then blocked in 5% skim milk. Membranes were incubated at 4°C overnight with specific antibodies, then incubated with horseradish peroxidase-conjugated anti-mouse IgG or anti-rabbit IgG (1:2000). After the membranes were washed, they were developed using the West-Q Chemiluminescent Substrate Kit Plus (GenDEPOT Inc., Barker, TX, USA). Intensities of the proteins were analyzed via Multi Gauge software (version 3.0, Fuji Photo Film, Tokyo, Japan).

*TPM1 transfection*

TPM1 plasmid DNA (OriGene Technologies Inc., Rockville, MD, USA) and Lipofectamine LTX (Invitrogen, Carlsbad, CA, USA) were used for transfection. One day before transfection, $1 \times 10^5$ SMC cells were plated in 6-well plates with M199 media. They were then incubated until reaching 50-60% confluence. Transfection was performed in accordance with reagent manufacturer instructions.

*Reverse transcription-polymerase chain reaction (RT-PCR)*

Total RNA was isolated with TRIzol Reagent (Invitrogen), then treated with DNase I. The RNA mixture was incubated at 95°C for 15 minutes before the first cycle and extended at 72°C for 10 minutes after all cycles were completed. A total of 30 cycles of amplification were performed. TPM1 primer sequences were as follows: Forward: 5'-CTCGCAGAAGGAAGACAGA-3' and reverse: 5'-ATTGGCACTTTGAATGGAAC-3.' The GAPDH control primer pair was obtained from BioSource International (Carlsbad, CA, USA). PCR products were separated by size on a 1% agarose gel in Tris-borate EDTA buffer. Band intensities were quantified using a densitometric scanner. Relative densities are expressed as ratios of control values.

*Flow cytometry*

SMCs ($1 \times 10^5$ cells) were seeded in 6-well plates and incubated in serum-free Opti-MEM for 24 hours before transfection. After transfection, SMC apoptosis was detected using the AnnexinV-FITC/PI apoptosis detection kit (BD Biosciences Pharmingen, San Diego, CA, USA), in accordance with manufacturer protocol. Briefly, SMCs were washed and resuspended in binding buffer and 5 μL fluorochrome-conjugated Annexin V was added to the 100 μL cell suspension. The SMC suspension was incubated for 15 minutes at room temperature in the dark. SMCs were washed and 5 μL propidium iodide staining solution was added to the cell suspension. The SMC suspension was incubated for 15 minutes at room temperature in the dark, then washed. The percentage of cell apoptosis was determined by flow cytometry using a BD LSRII flow cytometer (BD Biosciences, San Jose, CA, USA). All tests were performed in triplicate and repeated at least three times.

*Masson's trichrome staining*

Distributions of collagen and smooth muscles were assessed by staining with the Sigma-Aldrich HT15 kit (Sigma-Aldrich), in accordance with manufacturer protocol. All stained samples were captured using an Olympus fluorescence inverted microscope (200 × magnification).

*Statistical analyses*

Quantitative data are expressed as means ± standard deviation. Data were analyzed using Student's t-tests and correlation coefficients. *P*-values less than 0.05 indicate statistical significance. All statistical analyses were performed using Prism 5.01 for Windows (GraphPad Software, San Diego, CA, USA).

## Results

*Differential expression of collagen in megaureter*

Masson's trichrome staining was performed to investigate smooth muscle to collagen ratios. Expression of collagen was significantly increased in control ureters, while smooth muscle was visibly decreased in megaureters (**Figure 1A**, **1B**).

*Differential morphology of megaureter and control SMCs*

Primary cultured SMCs were stained with α-smooth muscle actin, comparing morpholo-

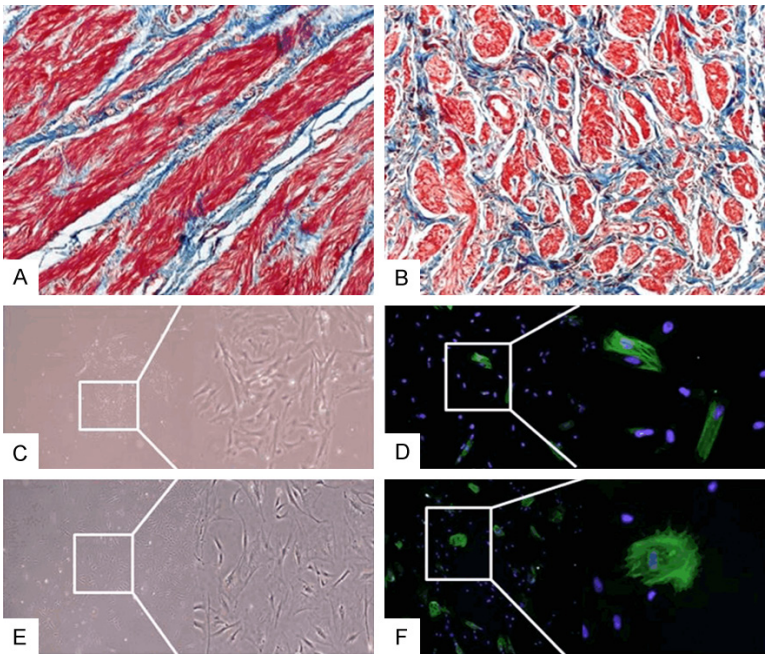


**Figure 1.** Fibrosis of megaureter tissues and α-smooth muscle actin staining of primary cultured SMCs. Ureter slide sections were stained with Masson's trichrome. Collagen is stained blue and muscle is stained red; (A) Control ureters show a normal smooth muscle layer; (B) The density of smooth muscle in megaureter was remarkably lower than that in control ureters. Primary cultured SMCs were stained with α-smooth muscle actin (green) and DAPI (blue); (C) SMCs of control ureter showed spindle-like and tapering shapes and (D) SMC actin was typical shape. (E) Megaureter SMCs appeared as spread shape cells and (F) a complicated pattern of filaments stretched out on all sides. Microphotographs were taken at 200 × magnification.

gies between megaureter and control cells. In the control group, SMCs showed spindle-like and tapering shapes, while megaureter SMCs exhibited a complicated pattern of filaments extending outward on all sides (**Figure 1C-F**).

*Two-dimensional gel electrophoresis and analyses of nanoflow LC-ESI-MS-MS*

Image analyses and quantification of 2D gel electrophoresis were performed with PDQuest software, version 8.0.1. Analyses of protein spots revealed more than 100 protein spots between megaureter and control ureters (**Figure 2A**, **2B**). Twelve protein spots showed statistically significant differential expression between megaureter and control ureters. Four spots showed overexpression and eight spots showed under-expression in megaureters. Differentially-expressed protein spots were identified through nanoflow LC-ESI-MS-MS and database searches. Typtophanyl-tRNA synthetase, Annexin A2, and ATP synthase subunit beta showed lower expression in megaureters than in control ureters. Conversely, TPM1 and smooth muscle proteins showed higher expression in megaureters (**Table 1**). Some protein spots were unknown or unnamed proteins and could not be identified because of low abundance. TPM1 was one of the proteins selected for functional investigations of ureters.

*Comparison of TPM1 and smooth muscle protein expression between megaureter and control ureters*

Expression levels of TPM1 and smooth muscle proteins were significantly increased in 2D gels. Confirming protein expression levels, Western blotting was performed with antibodies against TPM1 and smooth muscle actin. TPM1 and SM actin both showed higher expression levels in megaureters than in control ureters (**Figure 2C**, **2D**), consistent with LC-ESI-MS-MS data (**Table 1**, **Figure 2**).

*Artificial overexpression of TPM1 protein levels in control SMCs*

RT-PCR analyses were performed to confirm increased mRNA expression levels of TPM1 in transfected SMCs. Quantification of PCR bands in stained agarose gels by scanning densitometry indicated that relative expression levels of TPM1 in transfected SMCs were significantly higher than those in control SMCs (**Figure 3A**). **Figure 3B** shows the graphic analyses of averaged data.

*Apoptosis in megaureters, transfected, and control SMCs*

Cell apoptosis was detected using flow cytometry. FACS was performed immediately after transfection. The proportion of cells in early or late apoptosis was 44.39% in the TPM1 overexpression group. Lower proportions of apoptotic

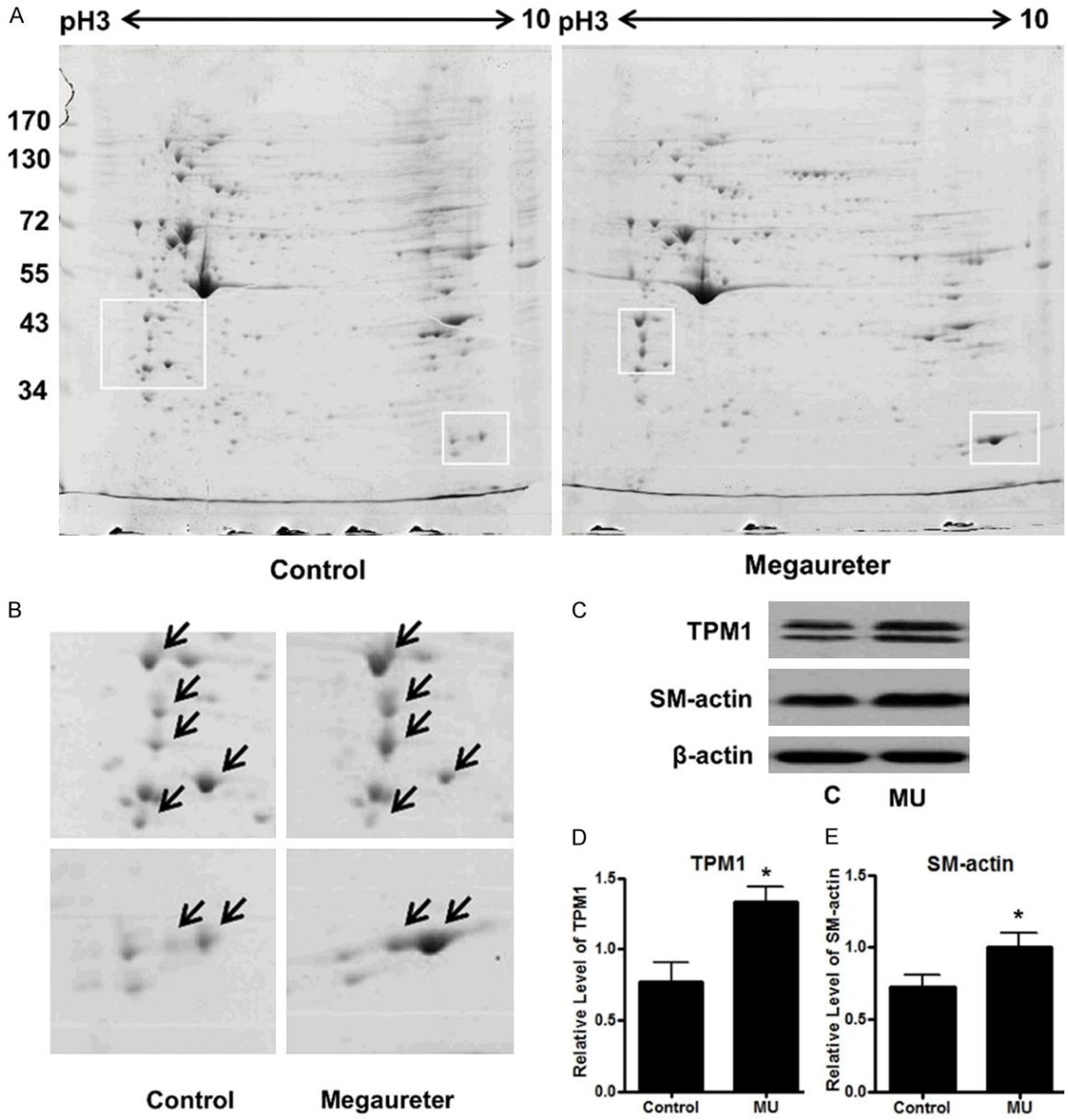


**Figure 2.** 2D analyses and TPM1 expression in primary cultured SMCs of megaureter and control ureters. Quantified proteins from SMCs were iso-electrically focused with an immobilized linear pH gradient and separated by 10% SDS-PAGE. Proteins were visualized by Coomassie blue staining; (A) Proteins in white boxes showed statistically significant differences in PDQuest analyses; (B) TPM1 and SM protein spots were expressed more strongly in megaureter SMCs than in control SMCs; (C) To confirm TPM1 and SM actin expression, Western blotting analyses were performed using proteins from both control and megaureter SMCs. TPM1 and SM actin were increased in megaureter SMCs, compared to control SMCs; Western blot gels were scanned with a densitometer to determine the areas under the bands. (D) TPM1 and (E) SM actin were significantly expressed in megaureter SMCs compared with the control group (*$P$-value < 0.05).

cells were observed in megaureter (27.4%) and control groups (10.7%), respectively. After 48 hours, nearly 70% of SMCs in the transfected group died. In contrast, a relatively high proportion of SMCs survived in the control group (**Figure 3C**, **3D**).

*Immunocytochemistry of TPM1 in control ureters and megaureters*

Control SMCs showed relatively weak expression of TPM1 and filaments with regular striations (**Figure 3E**). Shapes of SMCs and expres-

**Table 1.** Differentially-expressed protein spots between megaureter and control SMCs by nanoflow LC-ESI-MS-MS

| Spot no. | Protein ID | Accession no. | Score | MW (kD)/PI | Sequence coverage (%) |
|---|---|---|---|---|---|
| Under-expression | | | | | |
| 1 | Melanoma antigen | P78395 | 227 | 55.8/6.44 | 32 |
| 2 | ATP synthase subunit beta, mitochondrial | P06576 | 248 | 56.5/5.26 | 20 |
| 3 | Heterogeneous nuclear ribonucleoprotein C1/C2 | P07910 | 66 | 33.6/4.95 | 5 |
| 4 | Tryptophanyl-tRNA synthase, cytoplasmic | P23381 | 276 | 53.1/5.83 | 20 |
| 5 | Annexin A2 | P07355 | 356 | 38.5/7.57 | 70 |
| 6 | Guanine nucleotide-binding protein subunit beta-2 like | P63244 | 142 | 35.0/7.60 | 37 |
| 7 | Uncharacterized protein C15orf33 | Q96M60 | 19 | 59.9/9.00 | 0 |
| 8 | Unnamed protein | gi\|35844 | 80 | 49.8/4.66 | 8 |
| Overexpression | | | | | |
| 9 | Tropomyosin alpha-1 chain | gi\|63252896 | 78 | 32.7/4.71 | 16 |
| 10 | Nephronectin | Q6UXI9 | 38 | 61.8/8.74 | 0 |
| 11 | Transitional endoplasmic reticulum ATPase | P55072 | 174 | 89.2/5.14 | 10 |
| 12 | Smooth muscle protein | gi\|177175 | 64 | 22.5/8.56 | 25 |

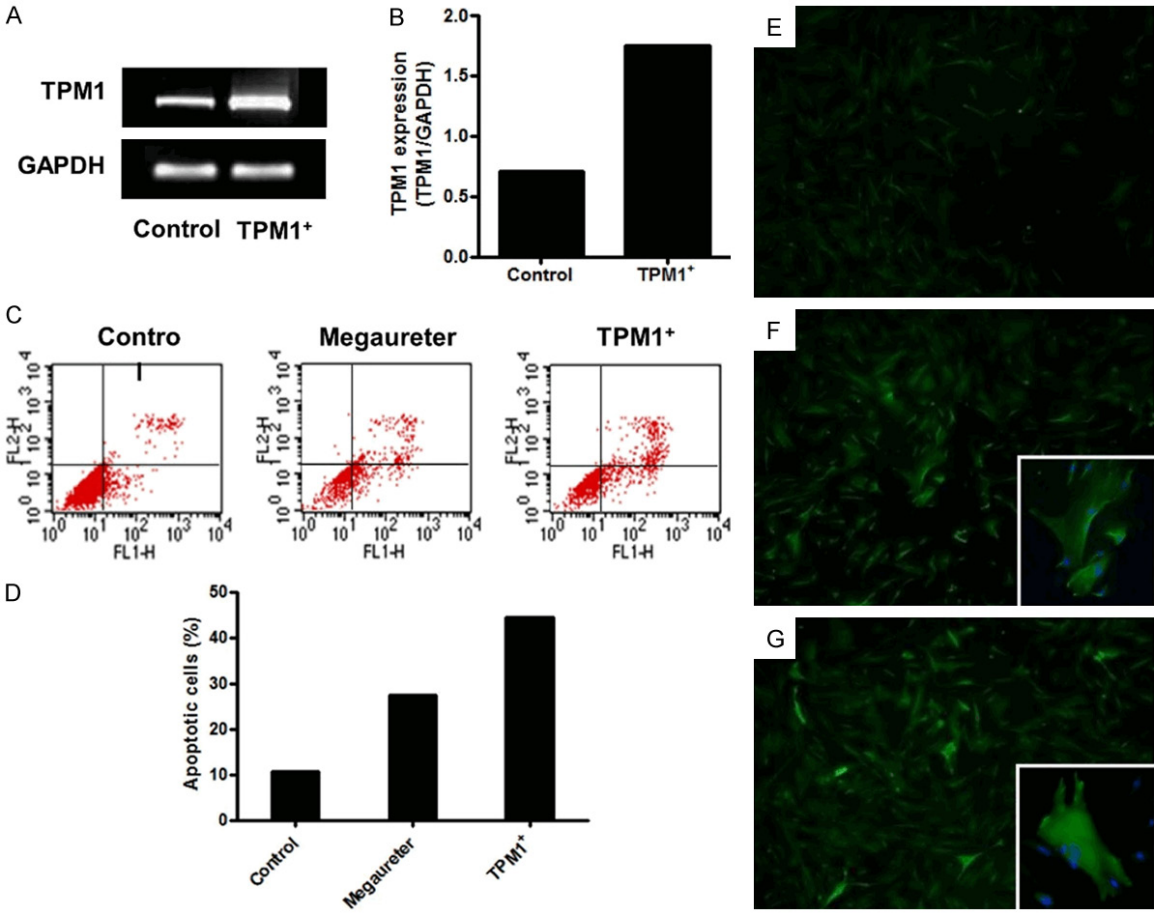


**Figure 3.** TPM1 expression and apoptosis analyses after TPM1 transfection. (A) TPM1 mRNA expression was greater in transfected SMCs than in control SMCs; (B) Expression of TPM1 protein was quantified by densitometric scanning of gels. Representative FACS data and bar graph summarizing the FACS results are shown; (C) The apoptosis rate was higher in the TPM1 overexpression and megaureter groups, compared to controls; (D) Bars represent the proportions of apoptotic cells in each group. Immunocytochemistry analyses show TPM1 expression (E) in normal SMCs, (F) in megaureter SMCs, and (G) in transfected SMCs. White arrows indicate focal adhesions. Microphotographs were taken at 100 × magnification.

sion levels of TPM1 differed in megaureters, compared to controls (**Figure 3F**). In megaureter SMCs, many brightly stained cells showed transformed shapes. Transfected SMCs showed the greatest increase in TPM1 expression levels. In particular, there were notable projections of focal adhesions (**Figure 3G**).

## Discussion

Ureteral distension and diameter are essential for maintenance of intraluminal pressure. Intraluminal pressure decreases with greater ureteral diameter. Excess collagen deposition has been presumed to play an important role in enlargement of the ureter [4, 11]. Increased collagen alters cell-to-cell junctions, thereby influencing myoelectrical propagation and peristalsis [4, 11]. Kajbafzadeh et al. demonstrated decreased muscular and increased collagen components, as well as an increased SMC apoptosis index, at the site of ureteropelvic junction obstruction [12]. However, Lee et al. reported no statistically significant differences in the proportion of collagen between megaureters and control ureters or in the ratio of collagen to muscle among subtypes of megaureter [13]. Thus, the current study attempted to identify the cause of megaureters, employing a proteomics approach. Proteomic methods using 2D and Nanoflow LC-ESI-MS-MS can analyze differential gene expression at the protein level, comparing the 2D patterns of proteins in control and megaureter SMCs. In analyses of protein spots, the current study found 20 protein spots that were differentially-expressed between megaureters and control ureters. TPM1, transitional endoplasmic reticulum ATPase, and smooth muscle proteins were significantly increased in megaureters, while melanoma antigen, mitochondrial ATP synthase subunit beta, cytoplasmic tryptophanyl-tRNA synthase, and annexin A2 were significantly decreased.

TPM1 is an actin binding protein that regulates cell motility and contractility. TPM1 makes actin filament compliant, which is associated with a two- to three-fold increase in the Vmax of the actin-activated ATPase activity of smooth muscle myosin. Mannikarottu et al. found that filament-associated proteins, including TPM1, enhance detrusor smooth muscle hypertrophy induced by partial bladder outlet obstruction [14]. Levels of thin filament-associated proteins (e.g., calponin, TPM, and caldesmon) are also increased in diabetic rabbit models [15]. The contractile properties of actin stress fibers may determine the structure of associated focal adhesions [16]. Creed et al. reported that TPM1 induces increased filopodia and generates a functionally distinct filament population [17]. Thus, the current study investigated TPM1 function using TPM1 plasmid DNA in control SMCs.

After TPM1 transfection, SMCs exhibited distinct morphological features. The edges of the SMCs (i.e., focal adhesions) were particularly more developed in TPM1 overexpressing cells. Furthermore, the expression rate of TPM1 was significantly reinforced in megaureter and transfected SMCs. The loss of actin stress fibers was related to cell transformation and metastasis. TPM1 stabilizes focal adhesions and inhibits cell migration. Raval et al. revealed that overexpression of high-molecular-weight TPM in transformed or tumor cells suppresses anchorage-independent cell growth, leading to anoikis [18]. The existence of anoikis is regulated by various factors, including integration signaling, focal adhesions, and cell-cell interactions [19]. In the present study, the rate of apoptosis was markedly increased in transfected and megaureter SMCs, compared to control SMCs. The proportion of apoptotic cells was nearly 50% in transfected SMCs, while the proportions were 27.4% and 10.7% in megaureter and control groups, respectively. Apoptosis of SMCs promotes tissue remodeling and repair via activation of cell migration, proliferation, and collagen synthesis [20]. Payabvash et al. discovered that muscular contents were reduced in obstructed vesicoureteral junctions, suggesting that the substitution of connective tissue may lead to functional obstructions in primary obstructive megaureters [21].

The present study compared expression levels of proteins in megaureter and control ureter SMCs via proteomic analyses. Although current results are unable to explain the underlying gene regulation pathways, they show that TPM1, a protein statistically overexpressed in megaureter SMCs, is a significant contributing factor in the development of obstructive megaureters.

## Conclusion

TPM1 was overexpressed in megaureter SMCs, compared to control ureter SMCs. As previously shown, increased expression of TPM1 alters the development of microfilaments and focal

adhesions. These changes may interrupt cell-cell and cell-matrix signal pathways, inducing anoikis of SMCs. Because of reduced migration of SMCs, the empty spaces left by dead cells are filled with connective tissue rather than myocytes. This may lead to the development of obstructive megaureters.

## Disclosure of conflict of interest

None.

**Address correspondence to:** Dr. Sang Won Han, Department of Urology, Urological Science Institute, Yonsei University College of Medicine, 134 Shinchon-Dong, Seodaemoon-Gu, Seoul 120-752, Korea. Tel: +82-2-2228-2310; Fax: +82-2-312-2538; E-mail: swhan@yuhs.ac

## References

[1] Zhong W, Yao L, Cui H, Yang K, Wang G, Xu T, Ye X, Li X and Zhou L. Laparoscopic ureteral reimplantation with extracorporeal tailoring and direct nipple ureteroneocystostomy for adult obstructive megaureter: long-term outcomes and comparison to open procedure. Int Urol Nephrol 2017; 49: 1973-1978.

[2] Choi YH, Cheon JE, Kim WS and Kim IO. Ultrasonography of hydronephrosis in the newborn: a practical review. Ultrasonography 2016; 35: 198-211.

[3] Tenkorang S, Omana JP, Mellas S, Tazi FM, El Ammari JE, Khallouk A, El Fassi MJ and Farih MH. Urolithiasis secondary to primary obstructive megaureter in an adult: a case report. J Med Case Rep 2017; 11: 177.

[4] Kang HJ, Lee HY, Jin MH, Jeong HJ and Han SW. Decreased interstitial cells of cajal-like cells, possible cause of congenital refluxing megaureters: histopathologic differences in refluxing and obstructive megaureters. Urology 2009; 74: 318-323.

[5] Winder SJ and Ayscough KR. Actin-binding proteins. J Cell Sci 2005; 118: 651-654.

[6] Gunning PW and Hardeman EC. Tropomyosins. Curr Biol 2017; 27: R8-R13.

[7] Squire JM, Paul DM and Morris EP. Myosin and actin filaments in muscle: structures and interactions. Subcell Biochem 2017; 82: 319-371.

[8] Wen LP, Fahrni JA, Troie S, Guan JL, Orth K and Rosen GD. Cleavage of focal adhesion kinase by caspases during apoptosis. J Biol Chem 1997; 272: 26056-26061.

[9] Janco M, Bonello TT, Byun A, Coster AC, Lebhar H, Dedova I, Gunning PW and Bocking T. The impact of tropomyosins on actin filament assembly is isoform specific. Bioarchitecture 2016; 6: 61-75.

[10] Hanash S. Disease proteomics. Nature 2003; 422: 226-232.

[11] Kart Y, Karakus OZ, Ates O, Hakguder G, Olguner M and Akgur FM. Altered expression of interstitial cells of Cajal in primary obstructive megaureter. J Pediatr Urol 2013; 9: 1028-1031.

[12] Kajbafzadeh AM, Payabvash S, Salmasi AH, Monajemzadeh M and Tavangar SM. Smooth muscle cell apoptosis and defective neural development in congenital ureteropelvic junction obstruction. J Urol 2006; 176: 718-723.

[13] Lee BR, Silver RI, Partin AW, Epstein JI and Gearhart JP. A quantitative histologic analysis of collagen subtypes: the primary obstructed and refluxing megaureter of childhood. Urology 1998; 51: 820-823.

[14] Mannikarottu AS, Disanto ME, Zderic SA, Wein AJ and Chacko S. Altered expression of thin filament-associated proteins in hypertrophied urinary bladder smooth muscle. Neurourol Urodyn 2006; 25: 78-88.

[15] Mannikarottu AS, Changolkar AK, Disanto ME, Wein AJ and Chacko S. Over expression of smooth muscle thin filament associated proteins in the bladder wall of diabetics. J Urol 2005; 174: 360-364.

[16] O'Neill GM. The coordination between actin filaments and adhesion in mesenchymal migration. Cell Adh Migr 2009; 3: 355-357.

[17] Creed SJ, Desouza M, Bamburg JR, Gunning P and Stehn J. Tropomyosin isoform 3 promotes the formation of filopodia by regulating the recruitment of actin-binding proteins to actin filaments. Exp Cell Res 2011; 317: 249-261.

[18] Zheng Q, Safina A and Bakin AV. Role of high-molecular weight tropomyosins in TGF-beta-mediated control of cell motility. Int J Cancer 2008; 122: 78-90.

[19] Zhong X and Rescorla FJ. Cell surface adhesion molecules and adhesion-initiated signaling: understanding of anoikis resistance mechanisms and therapeutic opportunities. Cell Signal 2012; 24: 393-401.

[20] Yu H, Clarke MC, Figg N, Littlewood TD and Bennett MR. Smooth muscle cell apoptosis promotes vessel remodeling and repair via activation of cell migration, proliferation, and collagen synthesis. Arterioscler Thromb Vasc Biol 2011; 31: 2402-9.

[21] Payabvash S, Kajbafzadeh AM, Tavangar SM, Monajemzadeh M and Sadeghi Z. Myocyte apoptosis in primary obstructive megaureters: the role of decreased vascular and neural supply. J Urol 2007; 178: 259-264.